SUPPLEMENTARY INFORMATION

A Medium-Bandgap Small Molecule Donor Compatible with Both Fullerene and Unfused-Ring Nonfullerene Acceptors for Efficient Organic Solar Cells

Xianjie Chen,[a,c] Xueyan Ding,[c] Qian Zhang,*[,c] Di Wang,[b] Lingling Zhan,[b] Xinhui Lu,[e] Feifei Wu,[a] Zheng Xu,[d] Huayu Qiu,*[,c,d] Wanzhi Chen,*[,a] Chang-Zhi Li*[,b]

[a]Department of Chemistry, Zhejiang University, Hangzhou 310028, PR China

[b]MOE Key Laboratory of Macromolecular Synthesis and Functionalization, State Key Laboratory of Silicon Materials, Department of Polymer Science and Engineering, Zhejiang University, Hangzhou 310027, P. R. China

[c]College of Material, Chemistry and Chemical Engineering, Hangzhou Normal University, Hangzhou, 311121, P. R. China

[d]Key Laboratory of Organosilicon Chemistry and Material Technology of Ministry of Education, Hangzhou Normal University, Hangzhou, 311121, PR China

[e]Department of Physics, Chinese University of Hong Kong, New Territories, Hong Kong 999077, P. R. China

Corresponding Authors:

* E-mail: chenwzz@zju.edu.cn (W.C.); czli@zju.edu.cn (C.L.); hyqiu@hznu.edu.cn (H.Q.); qzhang@hznu.edu.cn (Q.Z.).

Contents

1. Characterization

^{1}H-NMR and ^{13}C-NMR spectra were recorded on a Bruker AVANCE 500 spectrometer. Mass spectra were measured on a Walters MALDI Q-TOF Premier mass spectrometry. The thermogravimetric analyses (TGA) and differential scanning calorimetric measurements (DSC) were carried out on a TA Q500 and a TA Q2000 instrument under nitrogen gas flow with a 10 ^{o}C min^{-1} heating rate, respectively. UV-vis absorption spectra were obtained with JASCO V-570 spectrophotometer. Cyclic voltammetry (CV) measurements were taken on a LK2005A electrochemical workstation in distilled CH_2Cl_2 solution with a conventional three-electrode configuration employing a glassy carbon electrode as the working electrode, a saturated calomel electrode (SCE) as the reference electrode, and a Pt wire as the counter electrode at room temperature. Tetrabutylammonium phosphorus hexafluoride (Bu_4NPF_6, 0.1 M) in CH_2Cl_2 was used as the supporting electrolyte, and the scan rate was 100 mV s^{-1}. Atomic force microscopy (AFM) images were performed on Multimode 8 atomic force microscope in tapping mode. The transmission electron microscopy (TEM) investigation was performed on JEM 2100F at 200 kV. The specimen for TEM measurement was prepared by spin casting the blend solution on ITO/PEDOT:PSS substrate, then floating the film on a water surface, and transferred to TEM grids. GIWAXS measurements were carried out with a Xeuss 2.0 SAXS/WAXS laboratory beamline using a Cu X-ray source (8.05 keV, 1.54 Å) and a Pilatus3R 300K detector. The incidence angle is 0.2^{o}.

2. Fabrication and characterization of OSC devices.

Organic solar cells were fabricated with the normal structure of ITO/PEDOT:PSS/DRC4TB:Acceptor/PFN-Br/Ag. The ITO coated glass substrates were cleaned by ultrasonic treatment in detergent, deionized water, acetone, isopropyl alcohol and alcohol under ultrasonication for 15 min each and subsequently dried by a nitrogen blow. A thin layer of PEDOT:PSS (Clevios P VP AI 4083, filtered at 0.45 μm) was spin-coated at 4000 rpm onto ITO surface. After baking at 140 °C for 20 minutes, the substrates were transferred into an argon-filled glove box. For the nonfullerene devices, the active layer was spin-coated from 20 mg mL^{-1} chloroform solutions with weight ratio of DRC4TB and HF-PCIC at 1.5:1, and then the substrates were annealed at 120 ^{o}C for 10 min. For the fullerene devices, the active layer was spin-coated

from 15 mg mL^{-1} chloroform solutions with weight ratio of DRC4TB and $PC_{71}BM$ at 1:0.8, and then the substrates were placed in a glass petri dish containing 100 μL chloroform for 60 s for solvent vapor annealing (SVA). Subsequently, PFN-Br solution (0.5 mg ml^{-1}, dissolved in methanol) was spin-coated at 3000 rpm. Finally, 100 nm Ag layer were deposited under high vacuum (<2×10^{-4} Pa). The effective areas of cells were 6 mm^2 defined by shallow masks.

The current density-voltage (*J-V*) curves of photovoltaic devices were obtained by a Keithley 236 measurement source. The photocurrent was measured under 1 sun, AM 1.5G irradiation using a Xenon-lamp-based solar simulator (Taiwan Enlitech) calibrated with a standard Si solar cell, and the light intensity was calibrated with a standard photovoltaic (PV) reference cell. The external quantum efficiency (EQE) spectra were measured with a Stanford lock-in amplifier 8300 unit.

The charge carrier mobilities of the blended films were measured using the space-charge-limited current (SCLC) method. Hole-only devices with an architecture of ITO/PEDOT:PSS/DRC4TB:Acceptor/Ag and electron-only devices with an architecture of ITO/ZnO/DRC4TB:Acceptor/PFN-Br/Ag were fabricated. The device characteristics were extracted by modeling the dark current under forward bias using the SCLC expression described by the Mott-Gurney law:

$$J = \frac{9\varepsilon_0\varepsilon_r\mu_0 V^2}{8L^3} \qquad (1)$$

where J is the current density, L is the film thickness of the active layer, μ_o is the hole or electron mobility, ε_r is the relative dielectric constant of the transport medium, ε_0 is the permittivity of free space (8.85×10^{-12} F m^{-1}). β is a constant for each device, which could be got by fitting the dark current using the equation. V (= V_{appl} - V_{bi}) is the internal voltage in the device, where V_{appl} is the applied voltage to the device and V_{bi} is the built-in voltage due to the relative work function difference of the two electrodes.

3. Materials and synthesis

Unless stated otherwise, all the solvents and chemical reagents were obtained commercially and used without further purification. All reactions were carried out using standard Schlenk techniques.

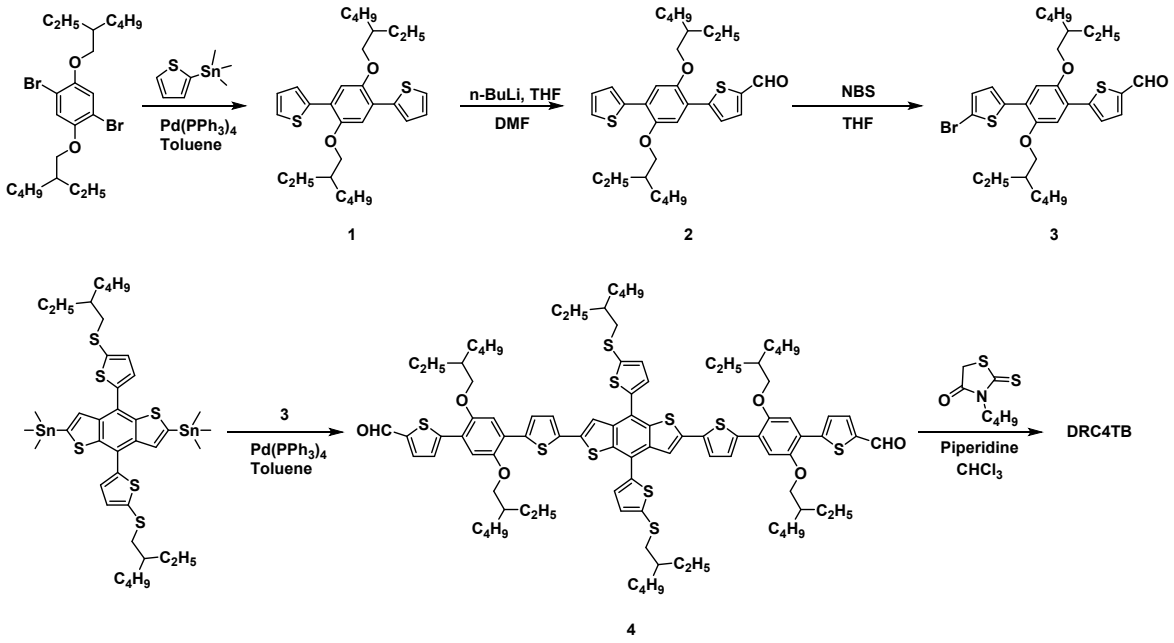

Scheme 1. Synthetic route of **DRC4TB**.

2,2'-(2,5-bis((2-ethylhexyl)oxy)-1,4-phenylene)dithiophene (**1**): A solution of 1,4-dibromo-2,5-bis((2-ethylhexyl)oxy)benzene (4.92 g, 10.0 mmol) and trimethyl(thiophen-2-yl)stannane (14.93 g, 40.0 mmol) in dry toluene (100 mL) was degassed twice with argon following the addition of $Pd(PPh_3)_4$ (4.62 g, 4.0 mmol). After stirring and refluxing for 24 h at 110 °C with the protection of argon, the reaction mixture was poured into water (100 mL) and extracted with dichloromethane (100 mL × 2). The organic layer was washed with water for twice and dried over anhydrous $MgSO_4$ for 3 h. The solvent was removed by evaporation under reduced pressure. The crude product was purified by silica gel column chromatography with dichloromethane/petroleum ether (1:5) as eluent to afford **1** as a pale-yellow solid (4.54 g, 9.1 mmol, 91%). ^{1}H NMR (500 MHz, $CDCl_3$) δ 7.61 (dd, J = 2.5, 1.2 Hz, 2H), 7.43 – 7.38 (m, 2H), 7.35 (d, J = 1.1 Hz, 2H), 7.17 (dd, J = 4.0, 1.0 Hz, 2H), 4.06 (d, J = 5.4 Hz, 4H), 1.92 (dt, J = 6.0 Hz, 2H), 1.64 (tdd, J = 7.3 Hz, 6H), 1.47 – 1.34 (m, 10H), 1.06 – 0.97 (m, 12H).

5-(2,5-bis((2-ethylhexyl)oxy)-4-(thiophen-2-yl)phenyl)thiophene-2-carbaldehyde (**2**): *n*-Butyllithium (1.3 mL, 3.10 mmol, 2.4 M) was added dropwise to a solution of **1** (1.4 g, 2.82 mmol) in THF (50 mL) at -78 °C with the protection of argon. After stirring at -78 °C for 3 h, DMF (0.26

mL, 3.38 mmol) was added dropwise to the reaction mixture at the same temperature. The solution was stirred at -78 °C for 30 min, and slowly warmed to room temperature. After stirring for 24 h, the reaction mixture was poured into water (100 mL) and extracted with dichloromethane (100 mL × 2). The organic layer was washed with water for twice and dried over anhydrous $MgSO_4$ for 3 h. The solvent was removed by evaporation under reduced pressure. The crude product was purified by silica gel column chromatography with dichloromethane/petroleum ether (1:1) as eluent to afford **2** as a yellow oil (1.26 g, 2.40 mmol, 85%).^{1}H NMR (500 MHz, $CDCl_3$) δ 9.84 (s, 1H), 7.67 (d, J = 4.0 Hz, 1H), 7.55 (d, J = 4.1 Hz, 1H), 7.49 (dd, J = 3.7, 0.9 Hz, 1H), 7.31 (dd, J = 5.1, 0.9 Hz, 1H), 7.21 (d, J = 2.6 Hz, 2H), 7.04 (dd, J = 5.1, 3.7 Hz, 1H), 3.93 (dd, J = 20.8, 5.6 Hz, 4H), 1.85 – 1.74 (m, 2H), 1.55 – 1.37 (m, 9H), 1.29 – 1.23 (m, 8H), 0.86 (ddd, J = 25.1, 10.6, 5.1 Hz, 12H).

5-(4-(5-bromothiophen-2-yl)-2,5-bis((2-ethylhexyl)oxy)phenyl)thiophene-2-carbaldehyde (**3**): NBS (0.42 g, 2.37 mmol) was added to the solution of **2** (1.13 g, 2.15 mmol) in dry THF (20 mL) in small portions with the protection of argon at 0 °C. After stirring 12 h at 25 °C in a dark environment, the reaction mixture was poured into water (100 mL) and extracted with CH_2Cl_2 (100 mL × 2). The organic layer was washed with water for twice and dried over anhydrous $MgSO_4$ for 3 h. The solvent was removed by evaporation under reduced pressure. The crude product was purified by silica gel column chromatography with dichloromethane/petroleum ether (1:1) as eluent to afford **3** as a yellow solid (1.07 g, 1.76 mmol, 82%). ^{1}H NMR (500 MHz, $CDCl_3$) δ 9.84 (s, 1H), 7.66 (d, J = 4.1 Hz, 1H), 7.54 (d, J = 4.1 Hz, 1H), 7.22 (d, J = 4.0 Hz, 1H), 7.19 (s, 1H), 7.14 (s, 1H), 6.98 (d, J = 4.0 Hz, 1H), 3.94 – 3.90 (m, 4H), 1.80 (dt, J = 12.2, 6.1 Hz, 2H), 1.52 – 1.43 (m, 6H), 1.27 (dt, J = 8.3, 5.6 Hz, 11H), 0.90 – 0.81 (m, 13H).

5,5'-(((4,8-bis(5-((2-ethylhexyl)thio)thiophen-2-yl)benzo[1,2-b:4,5-b']dithiophene-2,6-diyl)bis(thiophene-5,2-diyl))bis(2,5-bis((2-ethylhexyl)oxy)-4,1-phenylene))bis(thiophene-2-carbaldehyde) (**4**): A solution of **3** (634.0 mg, 1.05 mmol) and (4,8-bis(5-((2-ethylhexyl)thio)thiophen-2-yl)benzo[1,2-*b*:4,5-*b*']dithiophene-2,6-diyl)bis(trimethylstannane) (168.5 mg, 0.35 mmol) in dry toluene (100 mL) was degassed twice with argon following the

addition of $Pd(PPh_3)_4$ (127.1 mg, 0.11 mmol). After stirring and refluxing for 24 h at 110 °C with the protection of argon, the reaction mixture was poured into water (100 mL) and extracted with dichloromethane (100 mL × 2). The organic layer was washed with water for twice and dried over anhydrous $MgSO_4$ for 3 h. The solvent was removed by evaporation under reduced pressure. The crude product was purified by silica gel column chromatography with dichloromethane/petroleum ether (2:1) as eluent to afford **4** as a red solid (304.3 mg, 0.18 mmol, 51%).^{1}H NMR (500 MHz, CDCl3) δ 9.81 (s, 2H), 7.62 (d, J = 4.0 Hz, 2H), 7.52 (d, J = 4.9 Hz, 4H), 7.43 (d, *J* = 3.9 Hz, 2H), 7.29 (d, *J* = 3.6 Hz, 2H), 7.19 – 7.15 (m, 8H), 3.96 – 3.89 (m, 8H), 2.91 (d, *J* = 6.3 Hz, 4H), 1.80 (dt, *J* = 11.7, 5.9 Hz, 4H), 1.64 – 1.55 (m, 4H), 1.48 – 1.23 (m, 46H), 0.92 – 0.81 (m, 36H). ^{13}C NMR (126 MHz, CDCl3) δ 183.03, 150.13, 149.38, 149.28, 142.43, 141.77, 139.32, 138.62, 138.43, 137.92, 137.45, 137.34, 136.11, 132.36, 128.47, 126.76, 126.12, 125.31, 124.28, 122.74, 121.44, 118.30, 112.35, 111.58, 72.06, 71.98, 43.54, 39.78, 39.59, 39.35, 32.23, 30.74, 30.73, 29.21, 28.83, 25.45, 24.24, 24.14, 23.13, 23.09, 23.01, 14.17, 14.15, 11.46, 11.26, 10.91. MS (MALDI-TOF) *m/z*: calcd for $C_{98}H_{122}N_2O_6S_{10}$ 1692.6260; found, 1692.6487.

(5E,5'E)-5,5'-(((((4,8-bis(5-((2-ethylhexyl)thio)thiophen-2-yl)benzo[1,2-*b*:4,5-*b*']dithiophene-2,6-diyl)bis(thiophene-5,2-diyl))bis(2,5-bis((2-ethylhexyl)oxy)-4,1-phenylene))bis(thiophene-5,2-diyl))bis(methanylylidene))bis(3-butyl-2-thioxothiazolidin-4-one) (**DRC4TB**): **4** (135.4 mg, 0.08 mmol) and 3-butylrhodanine (129.0 mg, 0.80 mmol) was dissolved in a dry $CHCl_3$ (30 mL) under the protection of argon, and the three drops of piperidine was added to the mixture. After stirring and refluxing for 12 h, the mixture was extracted with dichloromethane (50 mL x 2), the organic layer was wash with water and dried over anhydrous $MgSO_4$ for 3 h. The solvent was removed by evaporation under reduced pressure. Then the crude product was purified by silica gel column chromatography with dichloromethane/petroleum ether (2:1) as the eluent to afford **DRC4TB** as a black solid (60.0 mg, 0.03 mmol, 35%). ^{1}H NMR (500 MHz, $CDCl_3$) δ 7.81 (s, 2H), 7.58 – 7.52 (m, 4H), 7.46 (s, 2H), 7.33 (d, *J* = 4.0 Hz, 2H), 7.30 (d, *J* = 3.4 Hz, 2H), 7.21 (s, 4H), 7.18 (s, 4H), 4.03 (dd, *J* = 16.8, 6.4 Hz, 8H), 3.96 (d, *J* = 4.3 Hz, 4H), 2.93 (d, *J* = 6.3 Hz, 4H). ^{13}C NMR (126 MHz, $CDCl_3$) δ 191.86, 167.07, 148.73, 148.33, 146.25, 140.78, 138.32, 137.50, 137.41, 136.82, 136.42, 136.26, 132.97, 131.32, 127.44, 125.52, 125.11, 124.67, 122.79, 121.60, 120.38, 118.55, 117.16, 110.18, 70.99,

47.64, 42.55, 38.80, 38.71, 38.31, 36.00, 31.19, 29.72, 29.67, 29.52, 28.69, 28.22, 27.79, 27.46, 24.41, 23.24, 23.10, 22.92, 22.09, 21.98, 13.17, 13.13, 13.11, 13.03, 10.49, 10.36, 9.86, 9.54. MS (MALDI-TOF) *m/z*: calcd for $C_{110}H_{140}N_2O_6S_{14}$ 2035.1780; found, 2034.6821.

4. Supplementary data

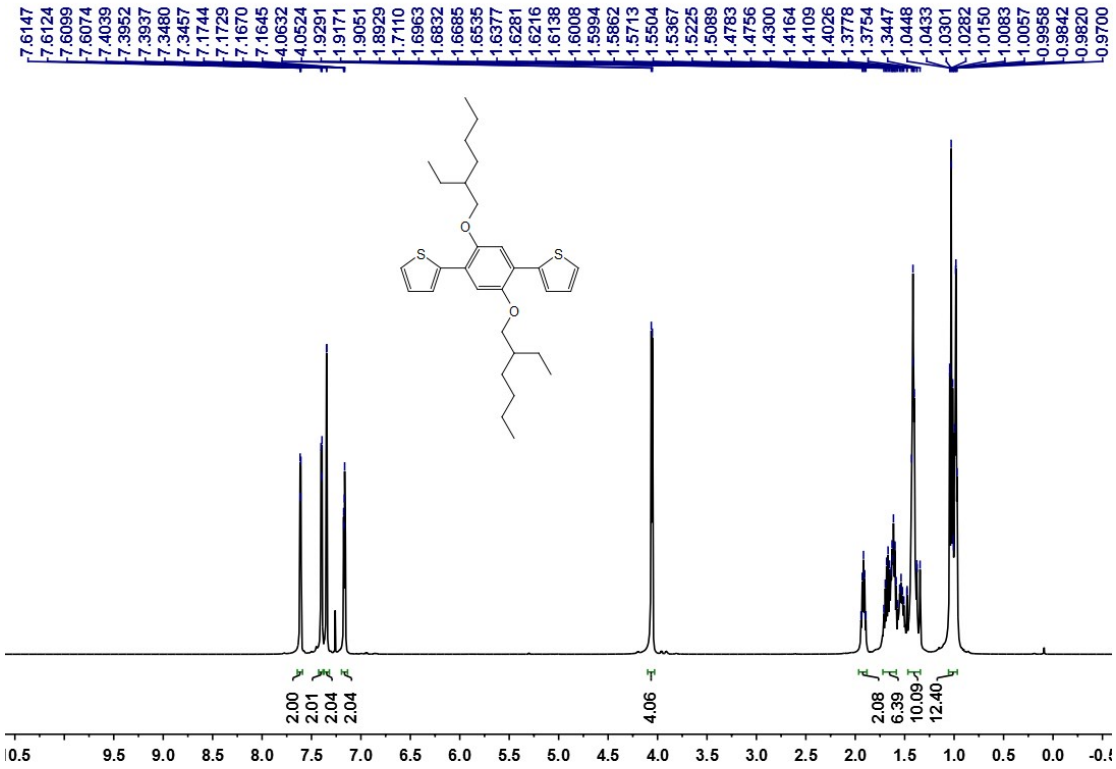

Figure S1. ^{1}H NMR spectrum of **1** at 293K in $CDCl_3$.

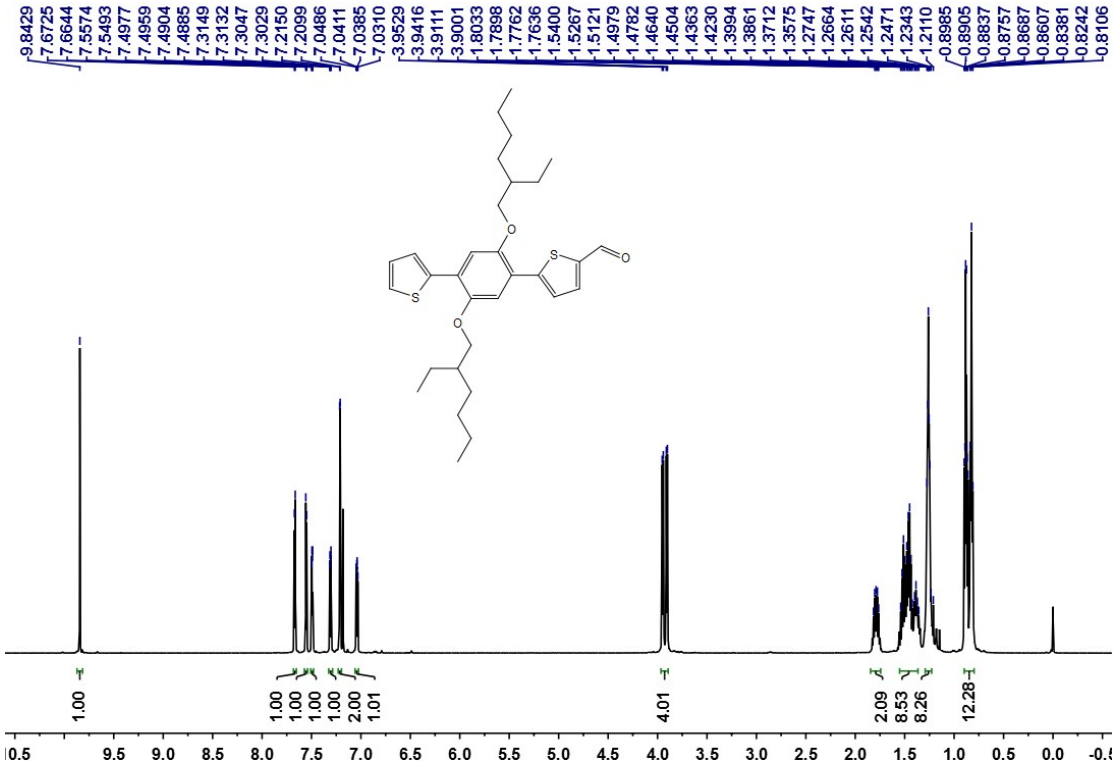

Figure S2. ^{1}H NMR spectrum of **2** at 293K in $CDCl_3$.

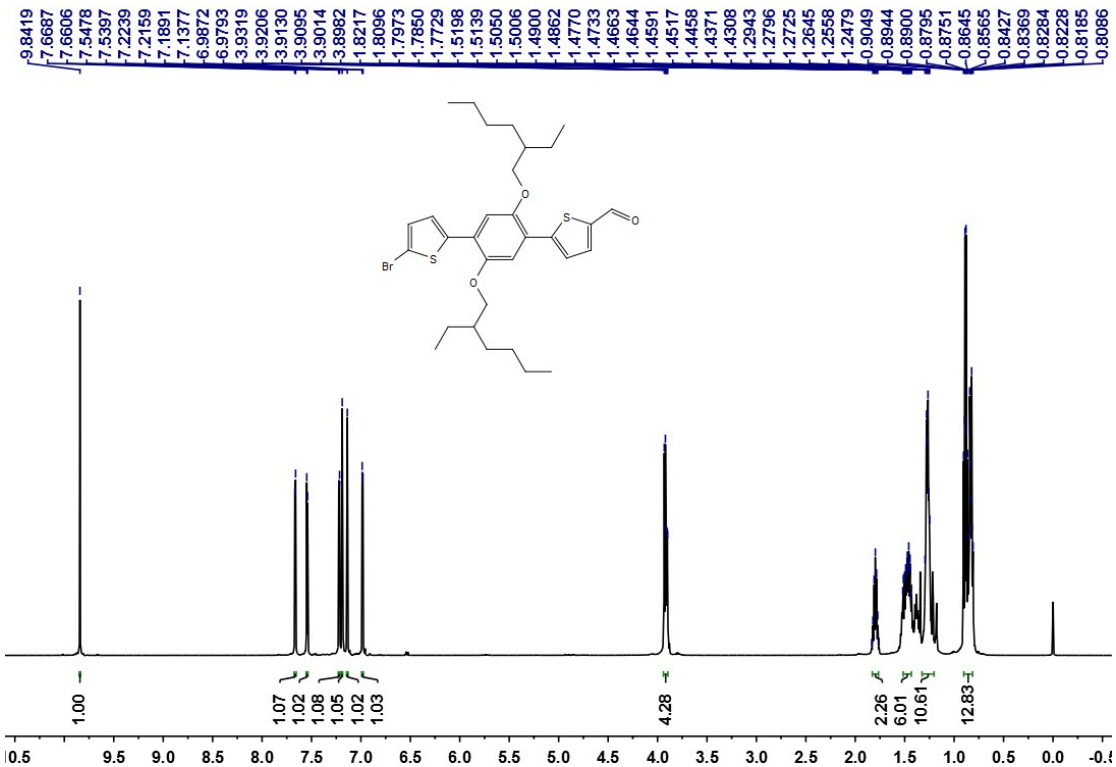

Figure S3. ^{1}H NMR spectrum of **3** at 293K in $CDCl_3$.

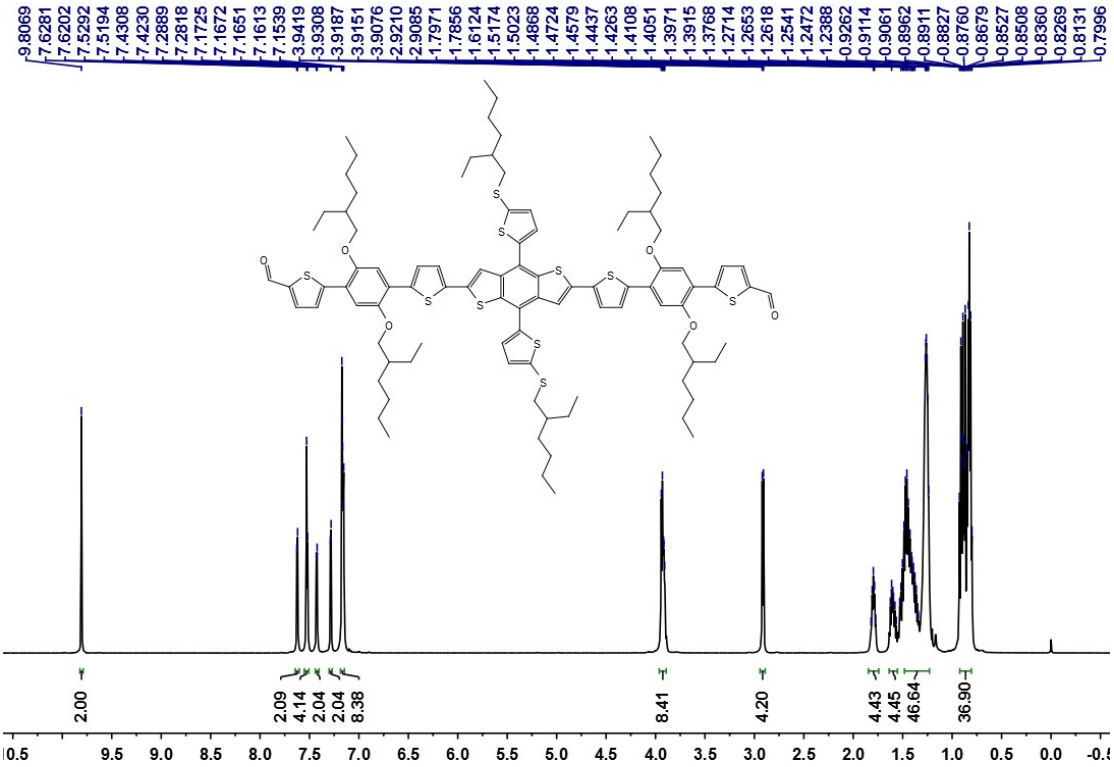

Figure S4. ^{1}H NMR spectrum of **4** at 293K in $CDCl_3$.

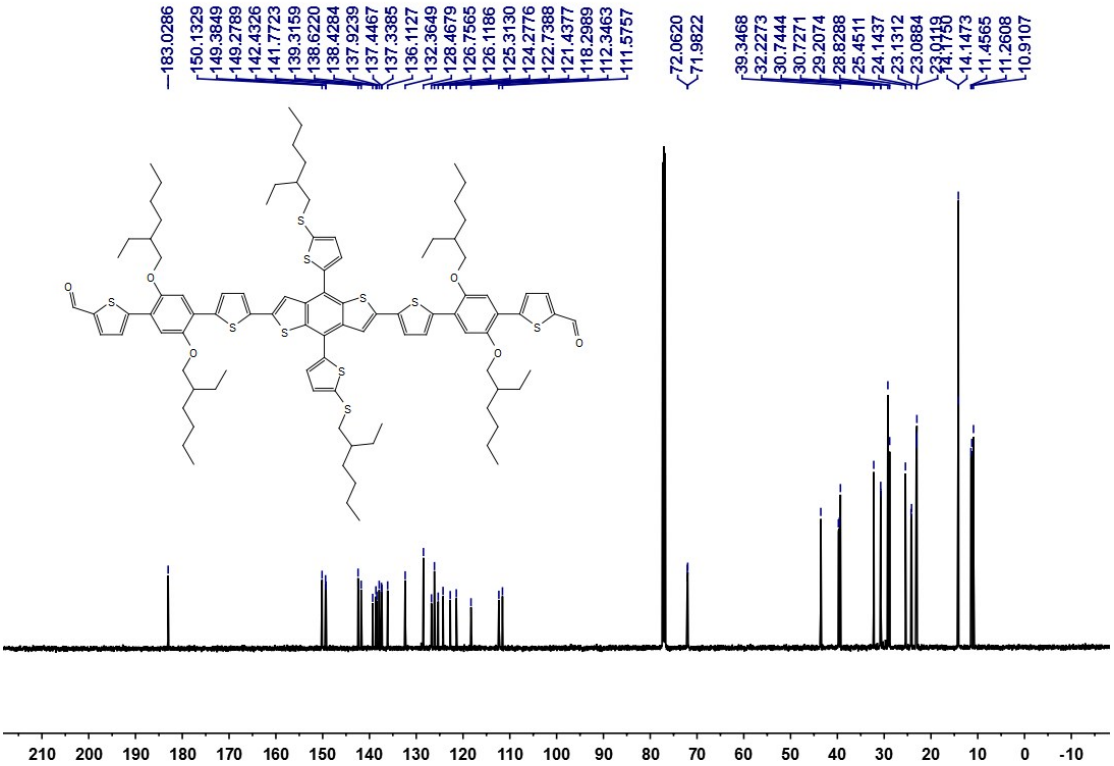

Figure S5. ^{13}C NMR spectrum of **4** at 293K in $CDCl_3$.

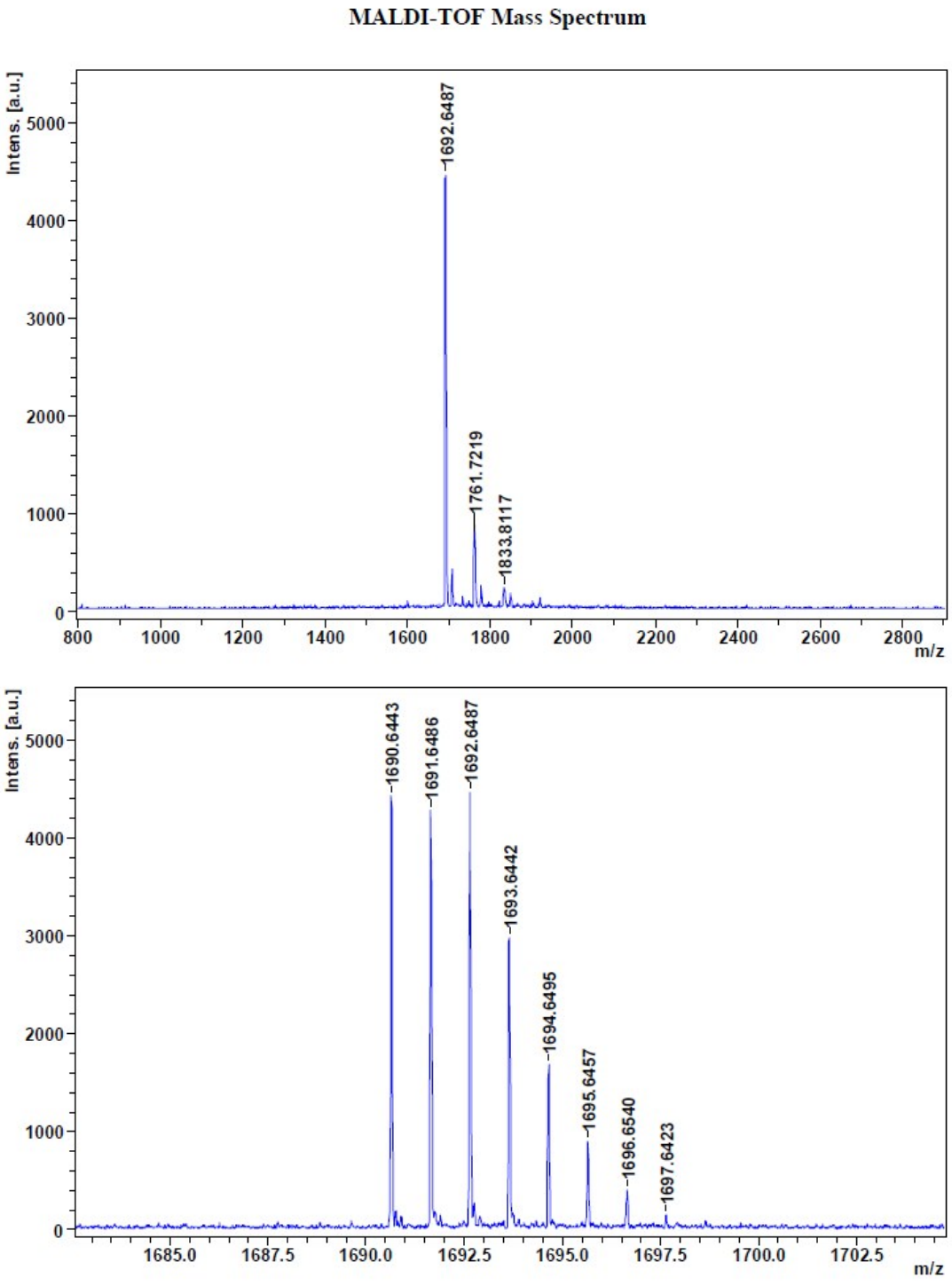

Figure S6. MALDI-TOF mass spectra of **4**.

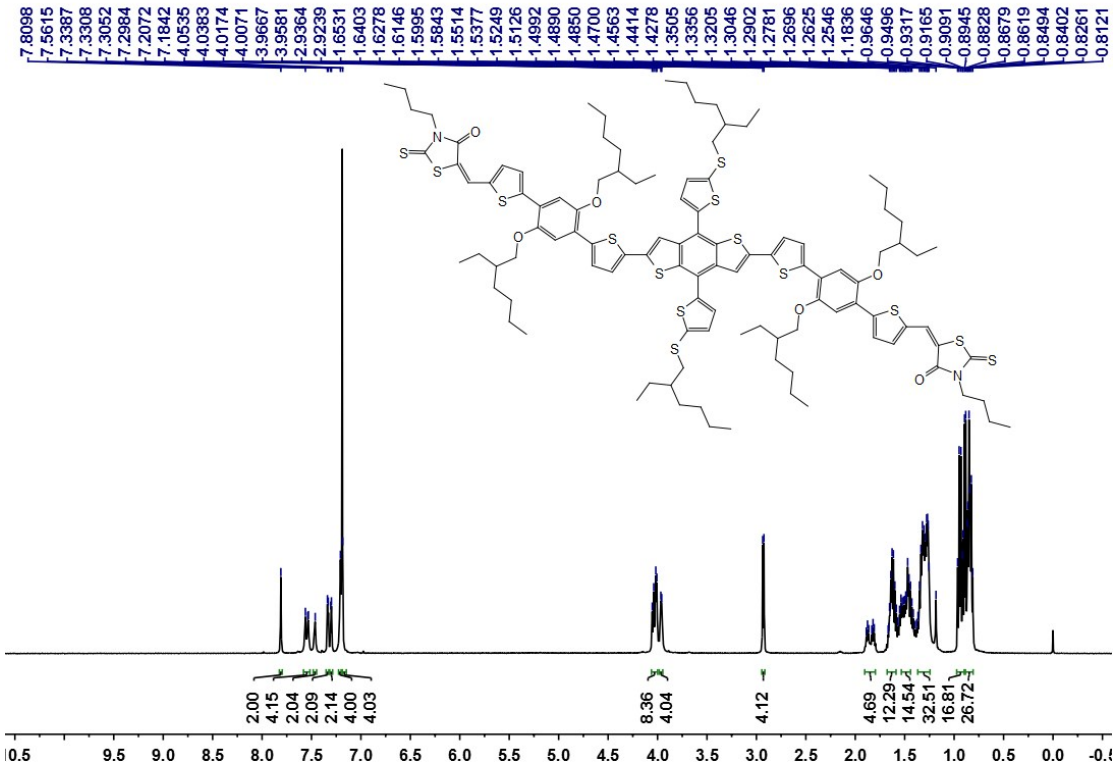

Figure S7. ^{1}H NMR spectrum of **DRC4TB** at 293K in $CDCl_3$.

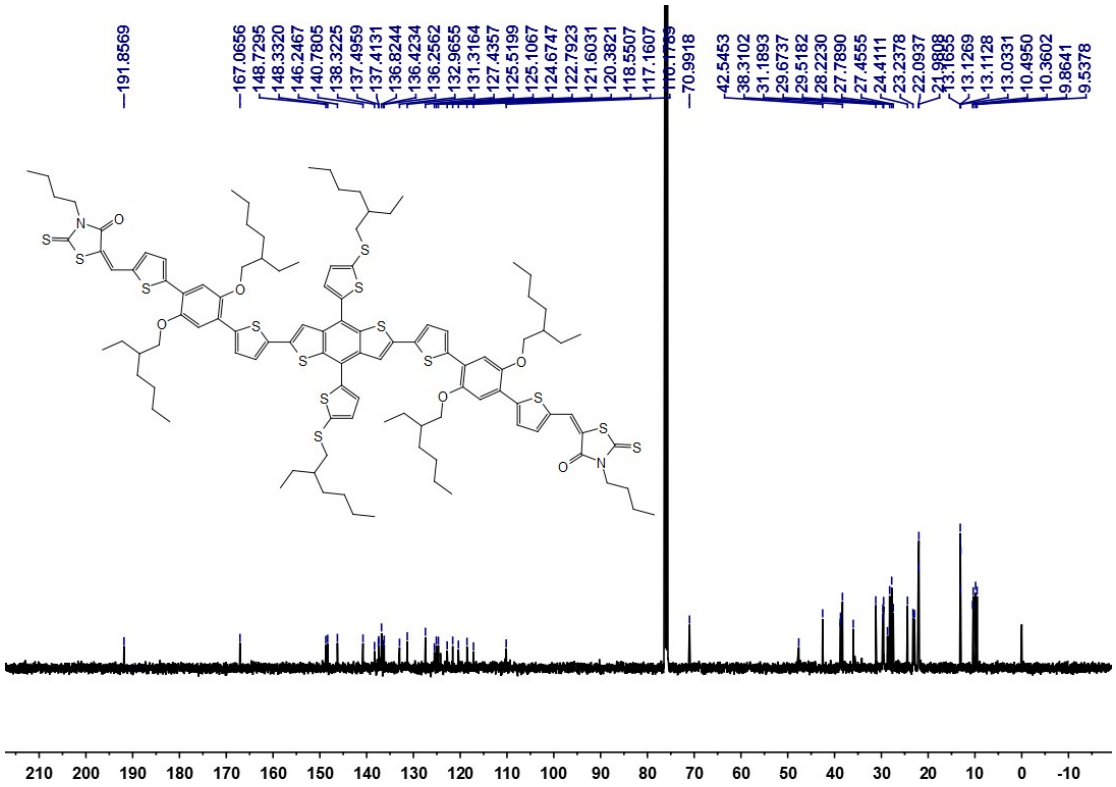

Figure S8. ^{13}C NMR spectrum of **DRC4TB** at 293K in $CDCl_3$.

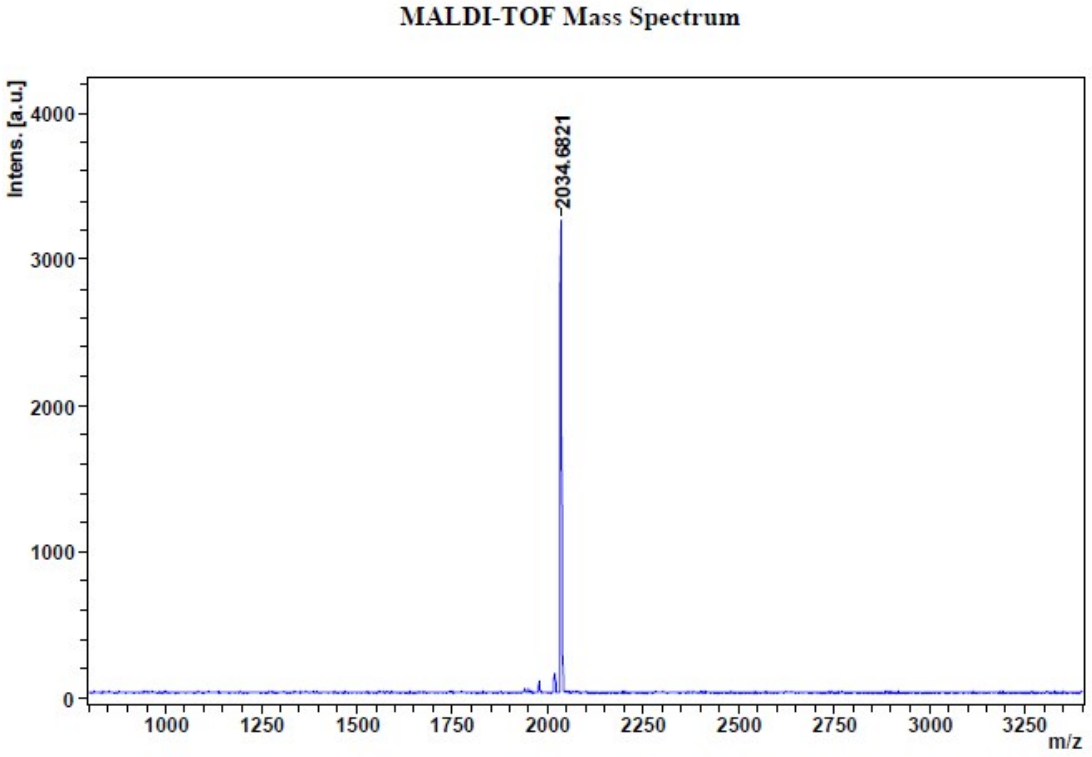

Figure S9. MALDI-TOF mass spectrum of **DRC4TB**.

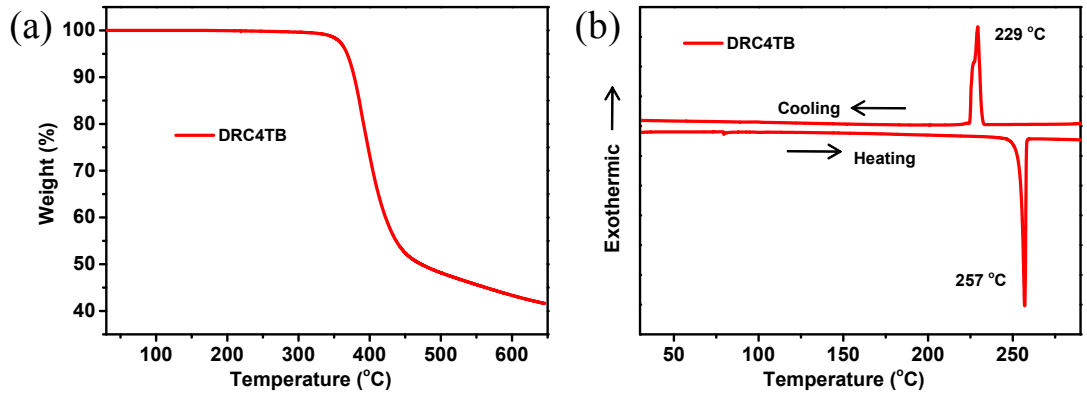

Figure S10. (a) TGA curve of DRC4TB; (b) DSC thermograms of DRC4TB with a heating rate of 10 ^{o}C min^{-1} under N_2. The lower lines and the upper lines are from the heating scans and cooling scans, respectively.

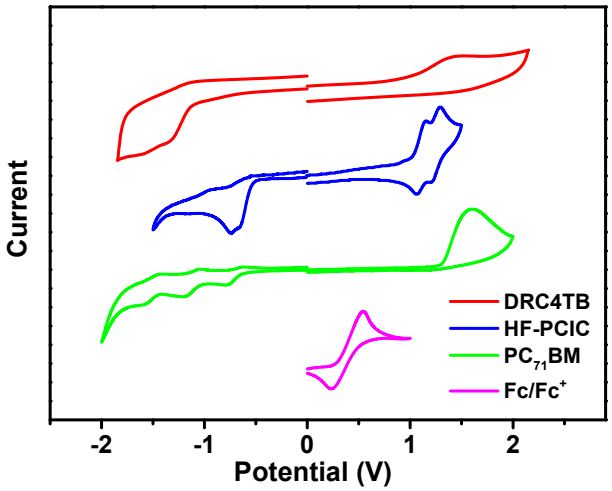

Figure S11. Cyclic voltammogram of DRC4TB, HF-PCIC, $PC_{71}BM$ and Fc/Fc^{+} in CH_2Cl_2 solutions of 0.1 mol L^{-1} Bu_4NPF_6 with a scan rate of 100 mV s^{-1}.

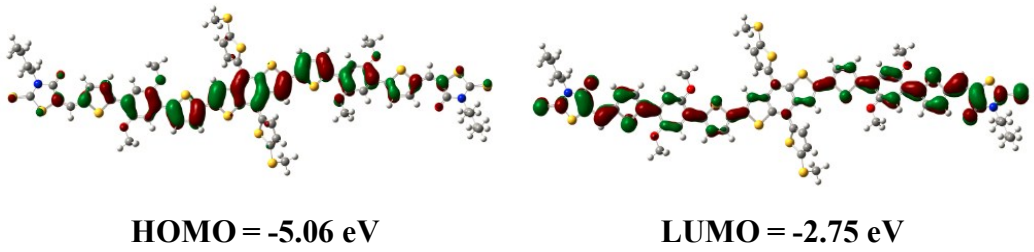

HOMO = -5.06 eV **LUMO = -2.75 eV**

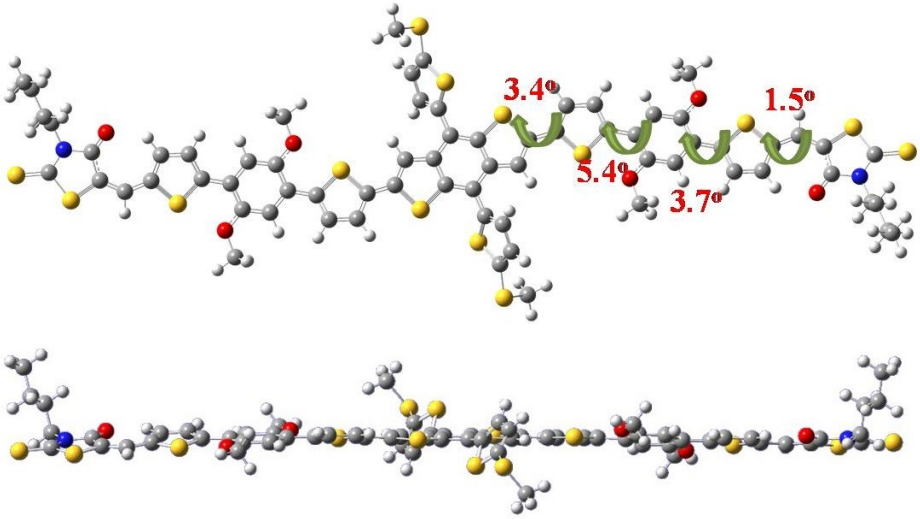

Figure S12. Electron density distribution of the frontier molecular orbitals and the optimized molecular geometries of DRC4TB using DFT evaluated at the B3LYP/6-31G(d) level. The ethylhexyl chains were replaced by methyl groups to reduce the computational time within a reasonable range.

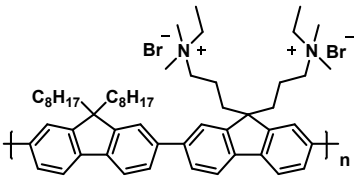

PFN-Br

Figure S13. Chemical structure of PFN-Br.

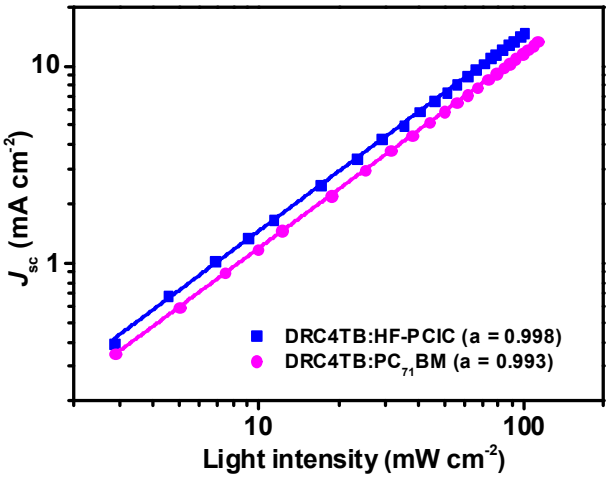

Figure S14. Dependence of J_{sc} on the light intensity (P_{light}) of the optimal nonfullerene- and fullerene-based devices.

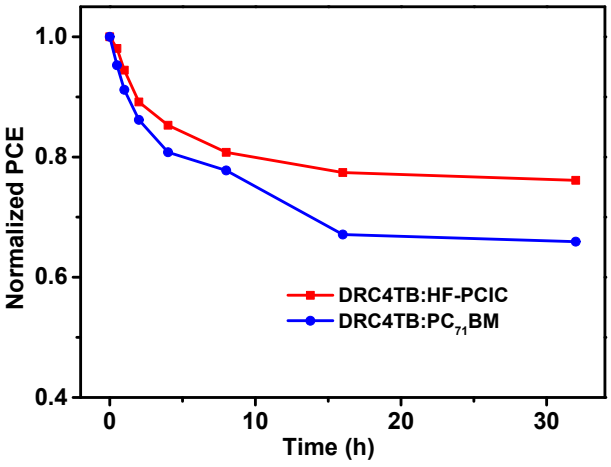

Figure S15. PCEs for the devices based on DRC4TB:HF-PCIC and DRC4TB:PC_{71}BM after thermal treatment at 80 °C for various times (Average data were obtained from 8 devices).

Table S1. Photovoltaic parameters of NFASM-OSCs with various D/A ratios after TA for 10 min (8 mg for donor in chloroform).

Weight ratio	V_{oc} (V)	J_{sc} (mA cm^{-2})	FF	PCE (%)
1.8:1	0.92	12.90	0.60	7.14
1.5:1	0.91	13.79	0.66	8.34
1.2:1	0.91	13.74	0.65	8.10
1:1	0.92	12.87	0.63	7.80
1:1.5	0.93	11.83	0.50	5.45

Table S2. Photovoltaic parameters of NFASM-OSCs with various concentration of DRC4TB after TA treatment for 10 min.

Concentration of donor (mg mL^{-1})	V_{oc} (V)	J_{sc} (mA cm^{-2})	FF	PCE (%)
8	0.91	13.79	0.66	8.34
10	0.91	14.97	0.62	8.41
12	0.91	15.51	0.62	8.68
14	0.90	15.61	0.58	8.16

Table S3. Photovoltaic parameters of NFASM-OSCs with various TA time and temperature.

Time (min)	Temperature (^{o}C)	V_{oc} (V)	J_{sc} (mA cm^{-2})	FF	PCE (%)
10	100	0.95	8.85	0.37	3.07
10	120	0.91	15.51	0.62	8.68
10	140	0.90	13.78	0.61	7.51

5	120	0.91	14.11	0.57	7.37
15	120	0.91	15.16	0.61	8.34

Table S4. Photovoltaic parameters of SM-OSCs with various D/A ratios after SVA (60 s) treatment (8 mg for donor in chloroform).

Weight ratio	V_{oc} (V)	J_{sc} (mA cm^{-2})	FF	PCE (%)
1.5:1	0.95	12.92	0.66	8.10
1.25:1	0.94	13.16	0.69	8.53
1:1	0.90	12.93	0.63	7.28
1:1.5	0.86	11.35	0.57	5.58

Table S5. Photovoltaic parameters of SM-OSCs with various concentration of DRC4TB after SVA treatment for 60 s.

Concentration of donor (mg mL^{-1})	V_{oc} (V)	J_{sc} (mA cm^{-2})	FF	PCE (%)
6	0.95	12.29	0.69	8.09
8	0.94	13.16	0.69	8.53
10	0.94	13.31	0.66	8.23

Table S6. Photovoltaic parameters of SM-OSCs with various SVA time.

SVA time	V_{oc} (V)	J_{sc} (mA cm^{-2})	FF	PCE (%)
30 s	0.95	11.96	0.61	6.90
45 s	0.95	12.79	0.61	7.37
60 s	0.94	13.16	0.69	8.53
75 s	0.94	13.01	0.54	6.56
90 s	0.94	12.44	0.52	6.03

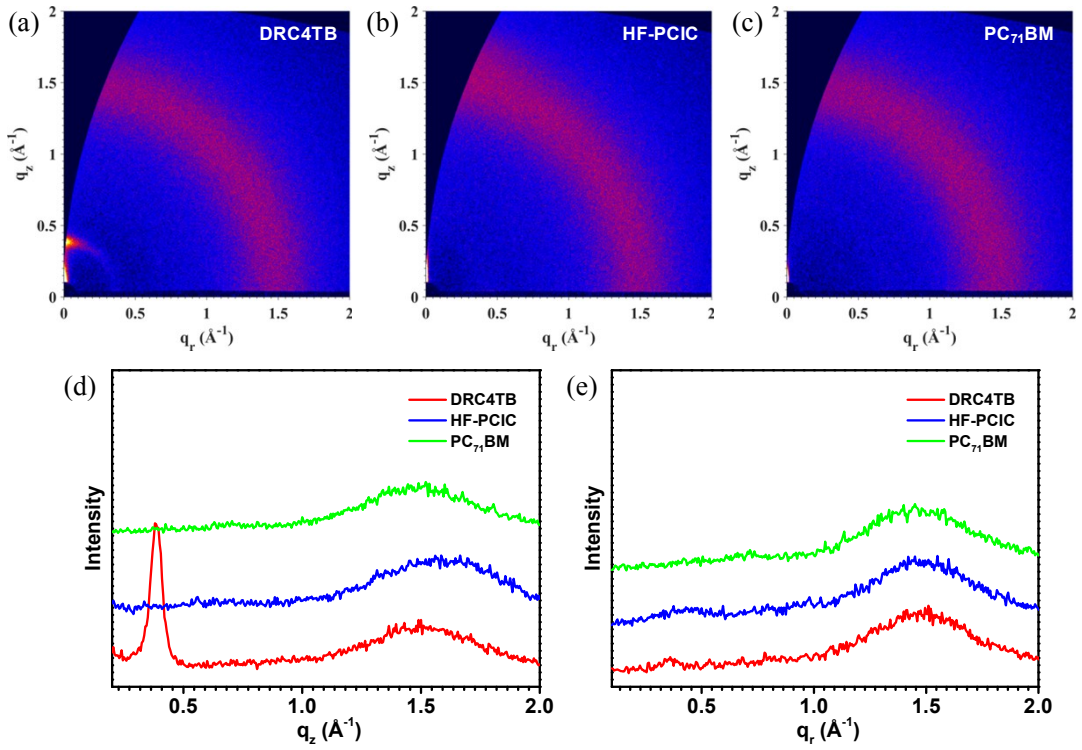

Figure S16. The 2D GIWAXS images of neat (a) DRC4TB, (b) HF-PCIC and (c) $PC_{71}BM$. The intensity profiles along (d) q_z and (e) q_r axis of the corresponding thin films.

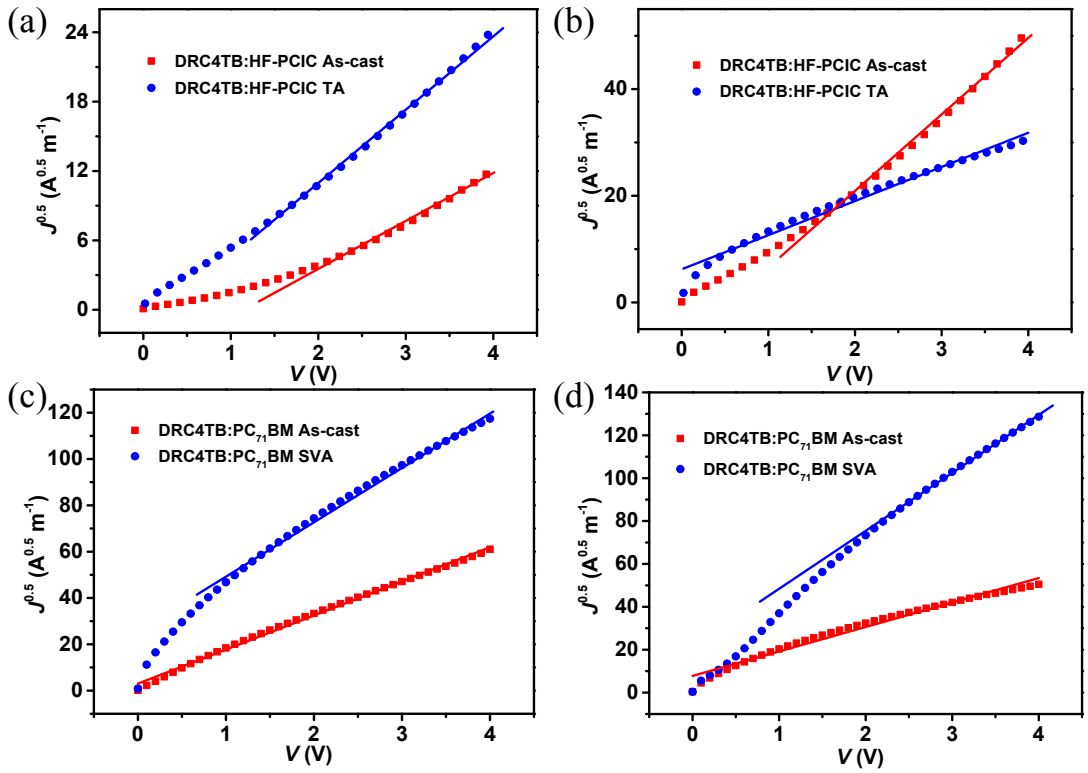

Figure S17. $J^{0.5}$-V curves of the hole-only devices based on (a) DRC4TB:HF-PCIC and (b) DRC4TB:PC_{71}BM. $J^{0.5}$-V curves of the electron-only devices based on (c) DRC4TB:HF-PCIC and (d) DRC4TB:PC_{71}BM.

Table S7. Hole/electron mobilities of DRC4TB:HF-PCIC and DRC4TB:PC_{71}BM blends under different conditions.

Blends	μ_h (10^{-4} cm^2 V^{-1} S^{-1})	μ_e (10^{-4} cm^2 V^{-1} S^{-1})	μ_h/μ_e
DRC4TB:HF-PCIC As-cast	0.06	0.47	0.13
DRC4TB:HF-PCIC TA	0.13	0.12	1.08
DRC4TB:PC_{71}BM As-cast	0.67	1.15	0.58
DRC4TB:PC_{71}BM SVA	2.39	3.27	0.73

5. References

(1) M. Zhang, X. Guo, W. Ma, H. Ade and J. Hou, *Adv. Mater.,* 2015, **27**, 4655-4660.